Confronting a mathematically derived constitutive law for the myocardium with experimental data

D. Caillerie[a], A. Mourad[b,c], and A. Raoult[b,*]

[a]*Laboratoire Sols, Solides, Structures, BP 53, 38041 Grenoble Cedex 9, France*
[b]*Laboratoire de Modélisation et Calcul, BP 53, 38041 Grenoble Cedex 9, France*
[c]*Bioengineering Institute, University of Auckland, PB 92019, New Zealand*

Abstract

The global myocardium contraction relies on the local deformation of its contractile cells. These small structures are rod-shaped and linked together by straight or Y-shaped junctions. A previous work introduced a discrete homogenization procedure that can be applied to the overall nonlinearly elastic lattice in order to derive an equivalent macroscopic constitutive law. Recent experimental measurements on cardiomyocytes allow us to give physiological grounds to the proposed method and to perform comparisons with well-known global laws.

Keywords: Myocardium; Lattice; Finite elasticity; Constitutive law; Discrete homogenization

1. Introduction

This paper is a sequel to Mourad et al. [1] which was presented at the Second MIT Conference on Computational Fluid and Solid Mechanics. In [1], we gave a brief description of the discrete homogenization procedure and explained the way it could, in principle, be used to derive a constitutive law for the myocardium seen as a repetitive structure. In the present work, we show that when we incorporate in the derivation of the homogenized constitutive law data arising from experimental measurements, we obtain results that are consistent with well-known macrosopic laws.

We first recall some modeling principles both in the framework of continuum mechanics and for elastic lattices. Then, we give a summary of the discrete homogenization procedure. We recall that it is aimed at providing a macroscopic constitutive law from the knowledge of the microscopical behavior. We emphasize the fact that the resulting law is not explicit. Finally, we use data due to Zile et al. [2] to define part of the mechanical properties of the microscopical elements of the network. We compare the resulting homogenized constitutive law with Lin and Yin's [3] law. Other comparisons have been performed with data due to Lacampagne [4].

* Corresponding author: Tel.: + 33 4 76 63 57 39; Fax: + 33 4 76 63 12 63; E-mail: annie.raoult@imag.fr

2. Macroscopic laws

The fibrous structure of the myocardium has long been recognized. In a simple purely hyper-elastic modeling (thus neglecting several effects), passive laws have to satisfy the principle of frame-indifference and the invariance around the fiber direction. Let us first recall the limitations such requirements impose on the energy density.

Let a reference configuration for an elastic body be given. From the frame-invariance, we know that the energy density is a function $W(x, \cdot)$ of the right Cauchy-Green tensor C. Following Spencer [5], some authors rewrite $W(x, \cdot)$ as a function of C and of $\tau \otimes \tau$ where τ is the fiber direction. We choose to follow the classical approach and to say that the existence of a preferred direction τ at point x means that all rotations with axis τ belong to the material symmetry group, or equivalently that:

$$\forall C \in \mathbb{S}_3^+, \forall Q \in SO(3) \tag{1}$$

such that

$$Q\tau = \tau, W(x, Q^T C Q) = W(x, C) \tag{2}$$

It is readily proved that the energy at point x reduces to a function of the three principal invariants of C and of the two extended invariants $\iota_4(C) = \tau \cdot C\tau$ and $\iota_5(C) = \tau \cdot C^2\tau$. The fourth invariant has a clear

Computational Fluid and Solid Mechanics 2005
K.J. Bathe (Editor)

geometrical meaning since it measures the fiber extension. No intuitive explanation of the fifth one seems to be given in the literature. Similarly, it cannot be reached in experimental measurements and it is classically omitted. Many constitutive laws for the myocardium have been proposed. We will concentrate here on Lin and Yin's [3] homogeneous law, which reads as follows for the passive myocardium:

$$W(C) = c_1(e^{Q(C)} - 1) \tag{3}$$

where

$$Q(C) = c_2(\iota_1(C) - 3)^2 + c_3(\iota_1(C) - 3)(\iota_4(C) - 1) + c_4(\iota_4(C) - 1)^2 \tag{4}$$

Experimental values have been obtained by these authors for seven rabbit specimens and are listed in Table 1.

Table 1
Experimental values in Lin and Yin's [3] law expressed in $\mathrm{g\,cm^{-2}}$

Rabbit specimen	1	2	3	4	5	6	7
c_1	1.01	2.42	9.86	2.92	2.62	1.67	6.85
c_2	3.05	12.13	4.62	3.21	2.40	1.70	2.88
c_3	−2.24	0.63	2.37	−2.60	−0.89	1.90	−0.76
c_4	1.92	1.05	0.09	2.01	2.01	0.38	0.38

3. Elastic lattices

In this section, we present a simple description of elastic lattices. Let us mention that the definitions we choose here for elastic laws for tensions and moments can be generalized. In particular, this formalism can be extended to graphene sheets modeling where more neighbors are taken into account.

3.1 Equilibrium

Let be given a lattice whose material elements consist of nodes $n \in \mathcal{N}$ and of bars $b \in \mathcal{B}$. The sets $\mathcal{N}$ and $\mathcal{B}$ can be seen as a reference configuration. The modeling Ansatz is that bars remain straight during deformation. In this context, external loads can be balanced by internal stresses $T^{\varphi}(b)$, which are functions of the bars, and by moments $M^{\varphi}(c)$, which are functions of the pairs of interacting bars (i.e. bars that meet in the same node). Submitted to loads $f^{\varphi}(n)$ that, for simplicity, act on nodes only, the lattice undergoes a one-to-one deformation $\varphi : \mathcal{N} \mapsto \mathbb{R}^3$. Assume, for simplicity again, Dirichlet boundary conditions on a subset $\mathcal{N}_0$. Letting $V = \{v : \mathcal{N} \to \mathbb{R}^3; \forall\, n \in \mathcal{N}_0,\, v(n) = 0\}$ and $\mathcal{N}_1 = \mathcal{N} \backslash \mathcal{N}_0$ the variational formulation of the equilibrium system reads:

$$\forall v \in V, -\sum_{b \in \mathbf{B}} T^{\varphi}(b) \cdot \Delta v(b) + \sum_{n \in \mathbf{N}_1} f^{\varphi}(n) \cdot v(n) = 0 \tag{5}$$

$$\forall \omega : B \mapsto \mathbb{R}^3, \; -\sum_{c \in C} M^{\varphi}(c) \cdot \nabla \omega(c) + \sum_{b \in \mathbf{B}} (\Delta \varphi(b) \wedge T^{\varphi}(b)) \cdot \omega(b) = 0 \tag{6}$$

where we make use of the discrete gradient notation for deformation or velocity vectors $\Delta v(b) = v(E(b)) - v(O(b))$, and for angular velocity vectors $\nabla \omega(c) = \omega(S(c)) - \omega(F(c))$, where $O(b)$ and $E(b)$ denote the origin and the end of bar b, and $F(c)$ and $S(c)$ denote the first and second bars of pair c. It can be noticed that if the axial components $T^{\varphi}_a(b)$ of the tension vectors and the moments are known, then so are the transverse components of the tension vectors by means of the above system.

3.2 Axiom of material indifference

This principle is the discrete analogue of the 3-D axiom of material indifference. It first states that stress vectors and moments rotate accordingly to a prescribed rigid body deformation. This reads

$$\forall Q \in SO(3), \forall q \in \mathbb{R}^3, \forall b \in B, \forall c \in C, T^{q+Q\varphi}(b) = QT^{\varphi}(b) \tag{7}$$

and

$$M^{q+Q\varphi}(c) = QM^{\varphi}(c) \tag{8}$$

Obvious evidence shows that, unlike 3-D bodies, lattices can undergo deformations that do not preserve orientation. It is then required that

$$\forall b \in B, \forall c \in C, T^{-\varphi}(b) = -T^{\varphi}(b) \tag{9}$$

and

$$M^{-\varphi}(c) = M^{\varphi}(c) \tag{10}$$

3.3. Elastic constitutive laws

We will say that a lattice is an elastic lattice if the local behavior of its mechanical components is governed by laws of the following form:

- there exists $\hat{N}^b : \mathbb{R}^3 \backslash \{0\} \mapsto \mathbb{R}$ such that $T^{\varphi}_a(b) = \hat{N}^b(\Delta\varphi(b))e^{\varphi}(b)$;
- there exists $\hat{M}^c : S^2 \times S^2 \mapsto \mathbb{R}$ such that $M^{\varphi}(c) = \hat{M}^c(e^{\varphi}(F(c)), e^{\varphi}(S(c)))$, where $e^{\varphi}(b)$ denotes the unit vector of $\Delta\varphi(b)$.

As previously mentioned, more complicated laws can be considered, for instance for graphene sheets. Let us

simplify even more by allowing an identical behavior to all bars and to all pairs of bars: $\hat{N}^b = \hat{N}$ independent of b and $\hat{M}^c = \hat{M}$. We can show that the axiom of material indifference is equivalent to the fact that the constitutive function $\hat{\mathrm{N}}$ resumes to a function depending on the Euclidean norm of the bars only, which means that

$$\forall z \in \mathbb{R}^3 \backslash \{0\}, \hat{N}(z) = \bar{N}(\|z\|) \tag{11}$$

and to the fact that the constitutive function $\hat{M}$ has the very specific following form:

$$\forall (z_1, z_2) \in S^2 \times S^2, \hat{M}(z_1, z_2) = \bar{M}(z_1 \cdot z_2) z_1 \wedge z_2 \tag{12}$$

Two features have to be underlined. First, in order to obtain Eq. (12), it is necessary to use Eqs. (9) and (10); Eqs. (7) and (8) by themselves are not sufficient. Second, it does not look surprising that, as stated by Eq. (12), moments are colinear to the wedge product of bars; this is actually a classical property. Nevertheless, we emphasize the fact that is not an Ansatz, but the consequence of material invariance.

3.4 Existence results

As soon as both constitutive laws satisfy the principle of material invariance, the system consisting of the equilibrium equations (5) and (6) can be equivalently written as the Euler–Lagrange equation of a minimization problem. More precisely, let W^b be a primitive of $\bar{N}$, let w be a primitive of $-\bar{M}$ and define $W^c(z_1, z_2) = w(\frac{z_1}{\|z_1\|} \cdot \frac{z_2}{\|z_2\|})$. Then, introduce the total energy

$$I(\varphi) = \sum_{b \in B} W^b(\Delta\varphi(b)) + \sum_{c \in C} W^c(\Delta\varphi(F(c)), (\Delta\varphi(D(c))) - \sum_{n \in N_1} f^\varphi(n) \cdot \varphi(n) \tag{13}$$

The derivative of I is given by

$$I'(\varphi)(v) = \sum_{b \in B} \hat{N}(\Delta\varphi(b)) \frac{\Delta\varphi(b)}{\|\Delta\varphi(b)\|} \cdot \Delta v(b) + \sum_{c \in C} M^\varphi(c) \cdot \nabla\omega(c) - \sum_{n \in N_1} f^\varphi(n) \cdot v(n) = 0 \tag{14}$$

where $\omega(b) = \frac{\Delta\varphi(b)}{\|\Delta\varphi(b)\|^2} \wedge \Delta v(b)$. Equation (14) is an equivalent form to Eqs. (5) and (6), once the transverse components of the tensions are eliminated. Assuming that N_0 is nonempty and choosing reasonable assumptions on the energies (for instance, there exist $\alpha > 0$ and $\alpha' \in \mathbb{R}$ such that $\forall b \in B$, $W^b(\|z\|) \geq \alpha \|z\|^2 - \alpha'$ and W^c is nonnegative), one can prove that I is coercive and that the minimization problem associated with I has a solution.

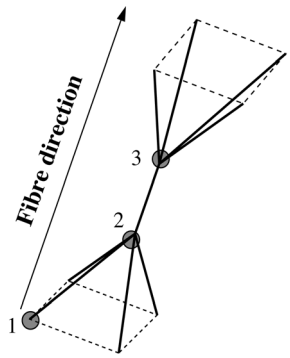

Fig. 1. Elementary pattern.

4. Homogenization procedure and resulting law

The homogenization procedure has been described at length in Caillerie et al. [6] and in Mourad [7]. It applies to lattices whose reference configurations are repetitive and whose bar lengths are small. In other words, we mean that there is an elementary reference brick made of $\mathcal{N}_R$ nodes and of $\mathcal{B}_R$ bars whose repetition along a given scale describes the whole of the lattice. Numerical simulations have been performed either with the elementary brick given in Fig. 1, for application to the myocardium, or with a Y-shaped brick, which generates a hexagonal lattice for application to carbon nanotubes. Following the general homogenization technique, we include a given lattice with aspect ratio – say ϵ – into a sequence of lattices indexed by ϵ whose sets of nodes are given by $\mathcal{N}^\varepsilon = \mathcal{N}_R \times Z^\varepsilon$ where $Z^\epsilon = \{\nu \in \mathbb{Z}^3, \epsilon\nu \in \omega\}$, ω being a given subset of $\mathbb{R}^3$, and we perform asymptotic expansions with respect to ε. The resulting equilibrium equations are, as expected, equations for a continuous medium; this is indeed the general motivation of homogenization techniques. However, the ouput we are actually interested in is the macroscopic constitutive law it provides.

This nonhomogeneous law is obtained in an implicit way. Let be given three vectors (G_1, G_2, G_3) in $\mathbb{R}^3$ which represent the deformation gradient G. From the whole development of the homogenization procedure, we have at our disposal a set of equations that provides the three stress vectors in $\mathbb{R}^3$ associated with G. This set of equations contains a nonlinear system, which, as customary in homogenization, is set on the reference brick. The number of its vectorial unknowns equals Card $\mathcal{N}_R$. It is solved by means of Newton's method.

For the validation of the homogenized law, we use experimental data obtained on isolated passive feline cardiomyocytes by Zile et al. [2] by means of a gel stretch method. Denoting by α the extension ratio of the cardiomyocyte and by σ the stress measured in $\mathrm{kN\,m^{-2}}$,

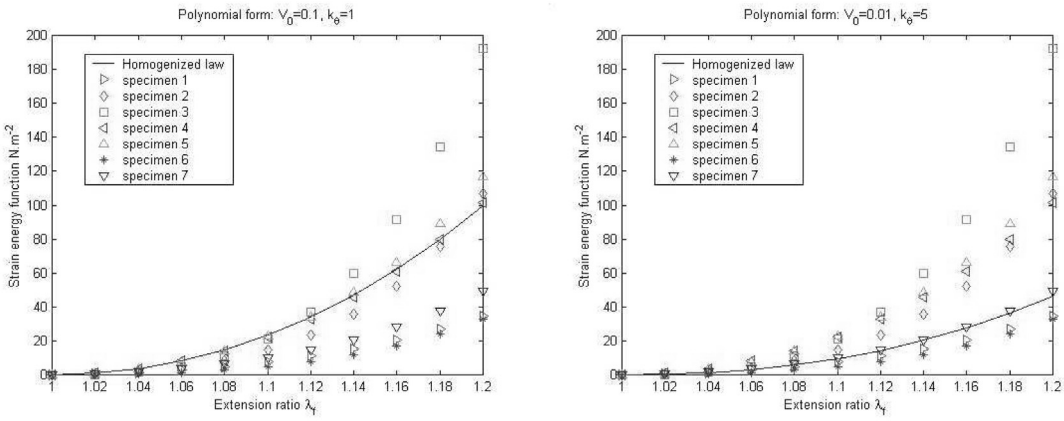

Fig. 2. Comparison with specimen 4 (left) and specimen 7 (right).

these authors suggest scalar laws $\sigma = \sigma(\alpha)$, where σ can be the polynomial function $\sigma = 300\,\alpha + 1020\,\alpha^2$ or the exponential function $\sigma = 14,5(e^{14,5\alpha} - 1)$. These two laws are actually really close for small α. These experimental data enter the framework of Eq. (11) by letting, for l_0 the length at rest and V_0 the cardiomyocyte volume,

$$\bar{N}(l) = \sigma\left(\frac{l - l_0}{l_0}\right)\frac{V_0}{l_0} \tag{15}$$

No experimental data on moments seem to be available and we use a simple law of the form $\bar{M}(z_1, z_2) = k_\theta(\theta - \theta_0)$, where θ_0 is the angle at rest between z_1 and z_2, and θ is the deformed angle.

5. Numerical results and discussion

Using the homogenized constitutive law (with fitted moment stiffness), we carried out numerical tests of uniaxial traction along the fiber direction, i.e. along the preferred direction of the reference brick, and we checked our results against values provided by Lin and Yin's [3] laws.

In Fig. 2, we plot the strain energy function with respect to the fiber extension ratio λ_f. The continuous line corresponds to the homogenized law, and the symbols correspond to Lin and Yin [3] experimental results. Good agreement is obtained. A next step could consist in performing comparisons between an homogenized law for an active state with experimental active laws. Such an attempt requires simulating mechanical data on activated isolated cardiomyocytes since actual experimental data seem to be lacking.

Acknowledgments

This work was supported by the Fonds National de la Science (ACI Modélisation mathématique, mécanique et numérique du myocarde) and by the Région Rhône-Alpes (Project Mathématique pour ADéMo).

References

[1] Mourad A, Caillerie D, Raoult A. A nonlinearly elastic homogenized constitutive law for the myocardium. In: Computational Fluid and Solid Mechanics, Oxford: Elsevier, 2003, pp. 1779–1781.
[2] Zile MR, Cowles MK, Buckley JM, Richardson K, Cowles BA, Baicu CF, Cooper G, Gharpuray V. Gel stretch method: a new method to measure constitutive properties of cardiac muscle cells. Am J Physiol 1998; 274:H2188–2202.
[3] Lin DHS, Yin FCP. A multiaxial constitutive law for mammalian left ventricular myocardium in steady-state barium contracture or tetanus. ASME, J Biomech Eng 1998;120:504–517.
[4] Lacampagne A. INSERM, Montpellier, private communication.
[5] Spencer AJM. Constitutive theory for strongly anisotropic solids. In: Spencer AJM, editor, Continuum Theory of the Mechanics of Fibre-Reinforced Composites. CISM Courses and Lectures 282. Wien: Springer Verlag, 1984, pp. 1–32.
[6] Caillerie D, Mourad A, Raoult A. Cell-to-muscle homogenization. application to a constitutive law for the myocardium. Math Model Num Anal 2003;37:681–698.
[7] Mourad A. Description topologique de l'architecture fibreuse et modélisation mécanique du myocarde. Doctoral dissertation, Institut National Polytechnique de Grenoble, 2003.